Mouse Model of Microembolic Stroke and Reperfusion

D.N. Atochin, MD, PhD; J.C. Murciano, PhD; Y. Gürsoy-Özdemir, MD, PhD; T. Krasik; F. Noda; C. Ayata, MD; A.K. Dunn, PhD; M.A. Moskowitz, MD; P.L. Huang, MD, PhD; V.R. Muzykantov, MD, PhD

Background and Purpose—To test the role of fibrinolysis in stroke, we used a mouse model in which preformed 2.5- to 3-μm-diameter fibrin microemboli are injected into the cerebral circulation. The microemboli lodge in the downstream precapillary vasculature and are susceptible to fibrinolysis.

Methods—We injected various doses of microemboli into the internal carotid artery in mice and characterized their distribution, effects on cerebral blood flow, neurological deficit, infarct area, and spontaneous dissolution. By comparing wild-type and tissue plasminogen activator (tPA) knockout ($tPA^{-/-}$) mice, we analyzed the role of endogenous tPA in acute thrombotic stroke.

Results—Microemboli cause dose-dependent brain injury. Although moderate doses of microemboli are followed by spontaneous reperfusion, they result in reproducible injury. Gene knockout of tPA markedly delays dissolution of cerebral emboli and restoration of blood flow and aggravates ischemic thrombotic infarction in the brain.

Conclusions—We describe a microembolic model of stroke, in which degree of injury can be controlled by the dose of microemboli injected. Unlike vessel occlusion models, this model can be modulated to allow spontaneous fibrinolysis. Application to $tPA^{-/-}$ mice supports a key role of endogenous tPA in restoring cerebral blood flow and limiting infarct size after thrombosis. **(*Stroke*. 2004;35:2177-2182.)**

Key Words: animal models ■ fibrinolysis ■ microemboli ■ stroke ■ stroke, embolic

Cerebrovascular occlusion by blood clots represents an important cause of morbidity and mortality.[1] Plasminogen activators like tissue plasminogen activator (tPA) and urinary plasminogen activator may restore cerebral perfusion and salvage brain tissue and function.[2] However, the role of endogenous plasminogen activators in stroke outcome is not known. In addition, the utility and safety of exogenous tPA in treatment of stroke remain to be more fully elucidated. While tPA may restore blood flow by fibrinolysis, it may also increase the risk of bleeding and may have direct neurotoxic effects.

We describe in this report a mouse model of acute cerebrovascular thrombosis in which we used preformed fibrin microemboli with mean diameter of 2.5 to 3 μm. Incorporation of ^{125}I-labeled fibrin into the microemboli provides quantitative information on deposition and dissolution of clots. After injection, microemboli form intravascular aggregates that lodge in the downstream precapillary vasculature. Tissue injury depends on microemboli concentration, which can be accurately dosed. In contrast, previous thromboembolic models used in the rat, rabbit, and mouse[3–5] use large (hundreds of microns in diameter) heterogeneous clot(s) that cannot be accurately dosed and do not reach the microvasculature.

We injected microemboli into the internal carotid artery (ICA) to produce dosed cerebral thrombosis by fibrinolysis-susceptible emboli. We characterized their deposition, dissolution, and effects on regional cerebral blood flow (rCBF), infarct size, and neurological outcome in normal and genetically modified mice. Our data indicate that microemboli can induce cerebral ischemia, leading to significant brain damage. The rate and extent of reperfusion and brain damage depend on the dose. Experiments in tPA knockout ($tPA^{-/-}$) mice suggest that endogenous tPA plays an important role in restoration of cortical cerebral blood flow (CBF).

Materials and Methods

Animals

Adult C57BL/6 mice (WT) and $tPA^{-/-}$ mice (Jackson Laboratory, Bar Harbor, Maine) weighing 20 to 30 g were used. All experiments were approved by the institutional animal care and use committees at University of Pennsylvania and Massachusetts General Hospital.

Received December 16, 2003; final revision received May 25, 2004; accepted May 26, 2004.

From the Cardiology Division and Cardiovascular Research Center (D.N.A., F.N., P.L.H.), Stroke and Neurovascular Regulation Laboratory, Department of Radiology (Y.G.-Ö., C.A., M.A.M.), and Athinoula A. Martinos Center (A.K.D.), Massachusetts General Hospital, Charlestown, Massachusetts; and the Institute for Environmental Medicine (J.C.M., T.K., V.R.M.) and the Department of Pharmacology (V.R.M.), University of Pennsylvania School of Medicine, Philadelphia, Pennsylvania.

Drs Atochin and Murciano contributed equally to this work as primary authors; Drs Huang and Muzykantov contributed equally to the experimental design as senior authors.

Correspondence to Dr Paul L. Huang, Cardiovascular Research Center, Massachusetts General Hospital East, 149 Thirteenth St, Charlestown, MA 02129. E-mail phuang1@partners.org

Stroke **is available at http://www.strokeaha.org** **DOI: 10.1161/01.STR.0000137412.35700.0e**

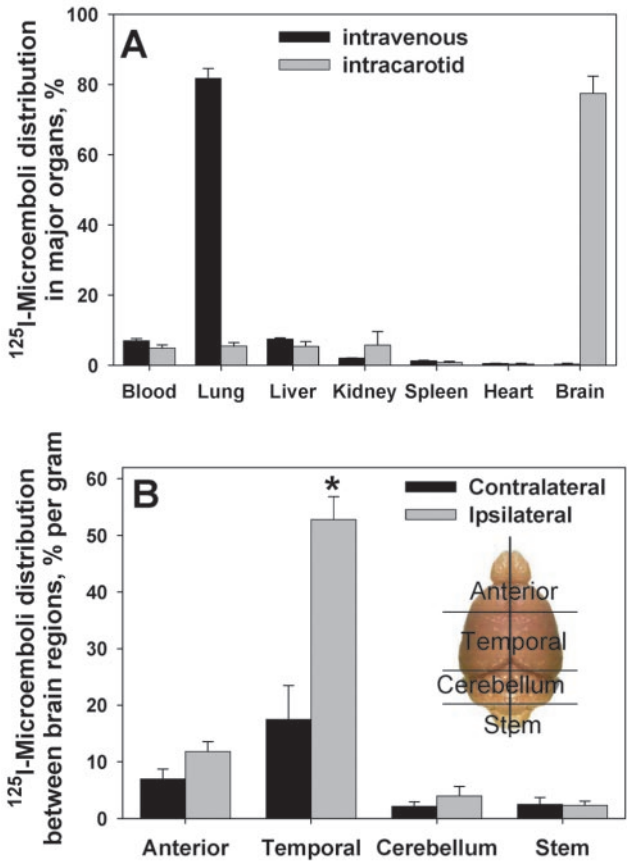

Figure 1. Tissue and brain distribution of microemboli. A, Tissue distribution of ^{125}I-labeled microemboli 10 minutes after intravenous (n=33) or intracarotid (n=6) injection in WT mice. B, Brain distribution of ^{125}I-labeled microemboli 10 minutes after intracarotid injection in WT mice (n=6). *$P<0.05$ vs contralateral side. Diagram shows the 4 regions in each hemisphere.

^{125}I-Labeled Fibrin Microemboli Distribution and Dissolution in Mice

Microemboli were prepared by adding thrombin (0.2 U/mL) to a fibrinogen solution (10 mg/mL).[6,7] After overnight maturation at 4°C, clots were dissected and homogenized. Radiolabeled microemboli were prepared by adding 20 μg of ^{125}I-labeled human fibrinogen before clot formation. Analysis with the use of a ZM Coulter Counter (Coulter Electronic, Ltd) showed that 1 μL of standard ^{125}I-labeled microemboli suspension contained 8100±750 microparticles, with an average diameter of 2.5 to 3 μm and an average total volume of microparticles of 5 to 10 μm^3. To determine tissue distribution, a bolus of radiolabeled microemboli was injected into the tail vein or the carotid artery. Animals were killed 10 minutes after injection to measure percent distribution of radioactivity in the blood and organs. In separate experiments, a bolus of radiolabeled microemboli was injected into the carotid artery to determine distribution within the brain. The brain was dissected into regions as shown in Figure 1B: anterior, temporal, cerebellum, and brain stem. Mice were killed at defined time points (10, 60, 180, and 300 minutes) after injection, and data were calculated as residual percentage of radioactivity recovered at the first time point.

Microembolic Stroke Model

Animals were anesthetized with 2% isoflurane and maintained with 1.5% isoflurane in 70% N_2O and 30% O_2 by facemask. Rectal temperature was maintained at 36.5±0.5°C with the use of a feedback-regulated heating system (FHC Inc). The left common carotid artery (CCA), external carotid artery (ECA), and ICA were exposed via a midline incision. A 6-0 silk suture was tied to the distal end of the ECA, and the left CCA, ICA, and pterygopalatine artery (PPA) were temporarily tied. A polyethylene catheter with inner diameter 0.02 mm was attached to a 1-mL syringe, introduced into the ECA, and secured with the 6-0 silk suture. The ligature around the ICA was removed, and the catheter was advanced into the lumen of the ICA. The microemboli solution was injected as a bolus into the ICA. The catheter was then withdrawn, and the ligature was removed from the CCA and PPA. To evaluate the effect of thrombotic burden on perfusion and brain injury, we used 3 doses of microemboli: small (4.0×10^5 particles), moderate (8.0×10^5 particles), and large (1.4×10^6 particles).

Filament Stroke Model

Permanent (24 hours) or transient (1 hour of ischemia, 24 hours of reperfusion) middle cerebral artery (MCA) occlusion (MCAO) was caused by inserting an 8-0 nylon filament covered by silicon into the ICA and advancing it to the origin of the MCA.[8]

Monitoring of rCBF by Laser-Doppler Flowmetry

CBF was determined by laser-Doppler flowmetry (LDF) with a fiberoptic probe (Perimed) attached to the skull 2 mm posterior and 6 to 7 mm lateral to bregma, measured along the surface of the skull (MCA territory). rCBF was measured before ICA ligation (100% baseline) and after injection of microemboli.

Laser Speckle Imaging

For laser speckle imaging (LSI), mice were placed in a stereotaxic frame, paralyzed with pancuronium bromide (0.4 mg/kg IV every 45 minutes), and ventilated (SAR-830 ventilator, Charles Ward Equipment) with monitoring of end-tidal CO_2. After reflection of the scalp, the skull surface was covered with a thin layer of mineral oil and diffusely illuminated with the use of a laser diode at 780 nm. The 5×4-mm imaging field of the charge-coupled device camera (Cohu) was positioned over the left hemisphere. Speckle contrast images were converted to images of correlation time values, which were assumed to be inversely proportional to rCBF.[6] Relative blood flow images were color coded for percentage of baseline, as described.[9]

Neurological Deficit Measurements

Neurological deficit measurements were performed at 24 hours after injection of microemboli, on a 5-point scale[10]: normal motor function was scored as 0, flexion of the contralateral torso and forelimb on lifting the animal by the tail as 1, circling to the contralateral side but normal posture at rest as 2, leaning to the contralateral side at rest as 3, and no spontaneous motor activity as 4.

Measurement of Infarct Volume

Animals were euthanized for infarct volume measurements 24 hours after microemboli injection or MCAO, immediately after scoring for neurological deficit. The volume of cerebral infarcts was measured with the use of Image analysis software (M4). With the use of an RMB-200C mouse brain matrix (Activation Systems), each brain was cut into 2-mm-thick coronal blocks, for a total of 6 blocks per animal. The tissue was immersed in 2,3,5-triphenyltetrazolium chloride (TTC) (Sigma) for 12 hours, which provides better contrast between normal and infarct zones than staining for 1 hour. The areas of infarction and each hemisphere were traced, and volumes were determined by integrating the appropriate area with the section thickness. The area of infarction in each section was expressed as a fraction of the nonischemic part of ipsilateral hemisphere (indirect volume of infarct). Measurements of infarct volumes and neurological deficits were performed in randomized-blind fashion.

Statistical Analysis

All data, except for neurological deficit measurements, are expressed as mean±SEM, and statistical analysis was performed with the use of *t* test comparisons. Differences of $P<0.05$ were considered

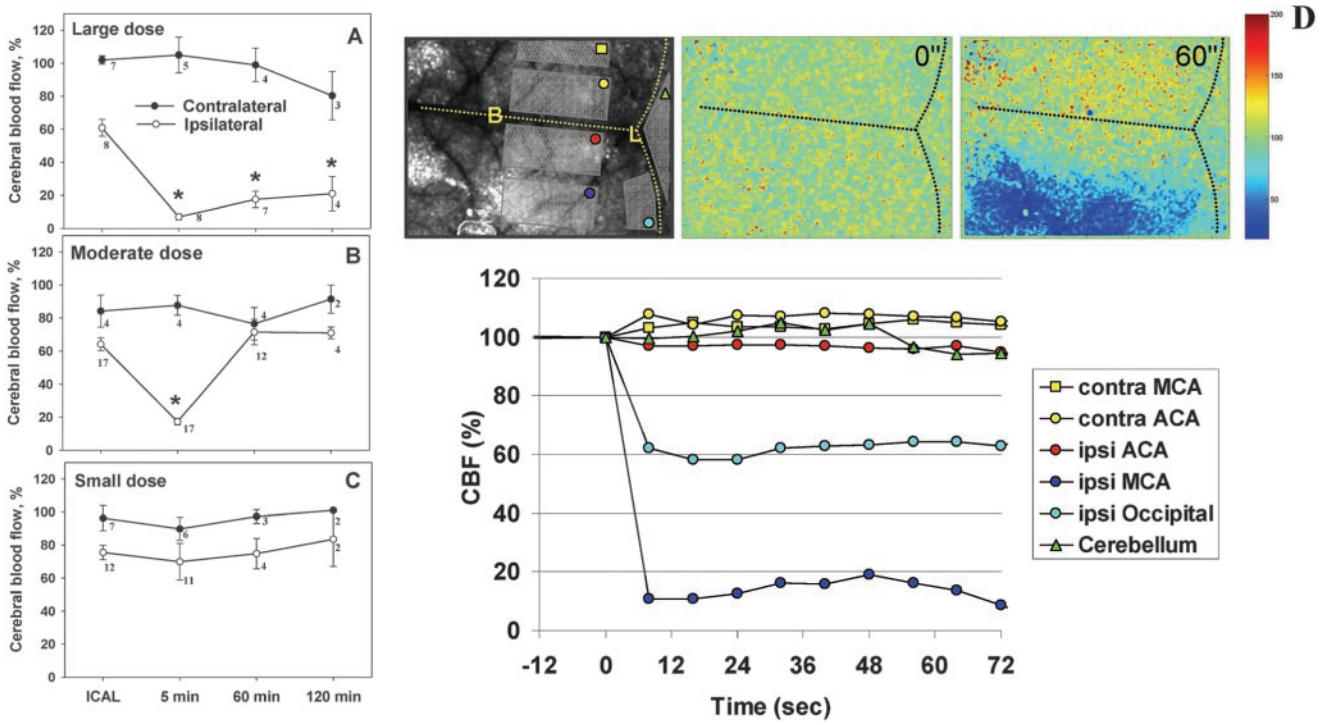

Figure 2. Effect of microemboli on rCBF. A to C, Time course of rCBF by LDF after ICA ligation (ICAL) and injection of microemboli. A, Large dose. B, Moderate dose. C, Small dose. Number of mice is indicated next to each data point. *$P<0.05$ vs contralateral side. D, Representative LSI during the first minute after left intracarotid injection of microemboli. Top left, Position of imaging field over the mouse head (B indicates bregma; L, lambda). Positions used to calculate rCBF in different arterial territories are shown. Top middle and top right, Speckle images at baseline (0") and 1 minute (60") after injection. Blood flow is mapped by a pseudocolor scale shown on the right. Bottom, Time course of rCBF changes.

significant. Neurological deficit data as seen in Figure 3F were analyzed with the Mann–Whitney test.

Results

Tissue and Brain Distribution of Microemboli

We compared the deposition of ^{125}I-labeled microemboli injected via the tail vein and the carotid artery. As seen in Figure 1A, intravenous injection deposited microemboli primarily in the lung, in agreement with previous data.[7] In contrast, intracarotid injection resulted in the major fraction of ^{125}I-labeled microemboli being lodged in the brain. After carotid injection, the major fraction of ^{125}I-labeled microemboli was localized in the temporal part in the ipsilateral hemisphere, although detectable amounts were found in the contralateral temporal hemisphere and other regions bilaterally (Figure 1B).

Effect of Microemboli on rCBF by LDF and LSI

The extent and duration of thrombotic occlusion and pathological consequences of microemboli depended on the dose of microemboli. Moderate and large doses of microemboli caused marked (≈80%) reductions of rCBF measured by LDF in the ipsilateral hemisphere by 5 minutes after injection, while small doses had little effect (Figure 2A, 2B, 2C). After a moderate dose, rCBF recovered to >60% by 1 hour, while it remained <20% with a large dose of microemboli.

We used LSI[9] to study the spatial distribution of ischemia induced by injection of microemboli. Small doses of microemboli caused a transient and variable rCBF reduction within the ipsilateral MCA territory (data not shown). Moderate doses of microemboli caused a more reproducible and severe reduction in rCBF in the ipsilateral MCA and, to a lesser extent, the PCA and ACA territories (Figure 2D).

Extent of Brain Damage by Microemboli

We compared the effects of intracarotid microemboli injection and MCAO by filament, a commonly used mouse model of stroke. A small dose of microemboli caused no significant injury. A moderate microemboli dose provided an intermediate extent of injury and caused a clearly detectable neurological deficit manifested by circling and depression of spontaneous activity. A large dose of microemboli led to a severe neurological deficit manifested by side positioning. Figure 3 shows the effects of microemboli dose on infarct size measured 24 hours later, images of representative brain sections, and neurological deficit scoring. Generally, the microembolic model of cerebral ischemia caused damage in the zone supplied by the MCA, but the affected areas also included other territories. The effects of the large dose of microemboli were similar to those of permanent MCAO by a filament.

The rate of postsurgical stroke-related death was paralleled by the size of infarcts. No animals died after injection of a small dose of microemboli, 10% died after a moderate dose, and 70% died after a large dose. In comparison, 13% died after transient filament MCAO, and 37% died after permanent MCAO by filament.

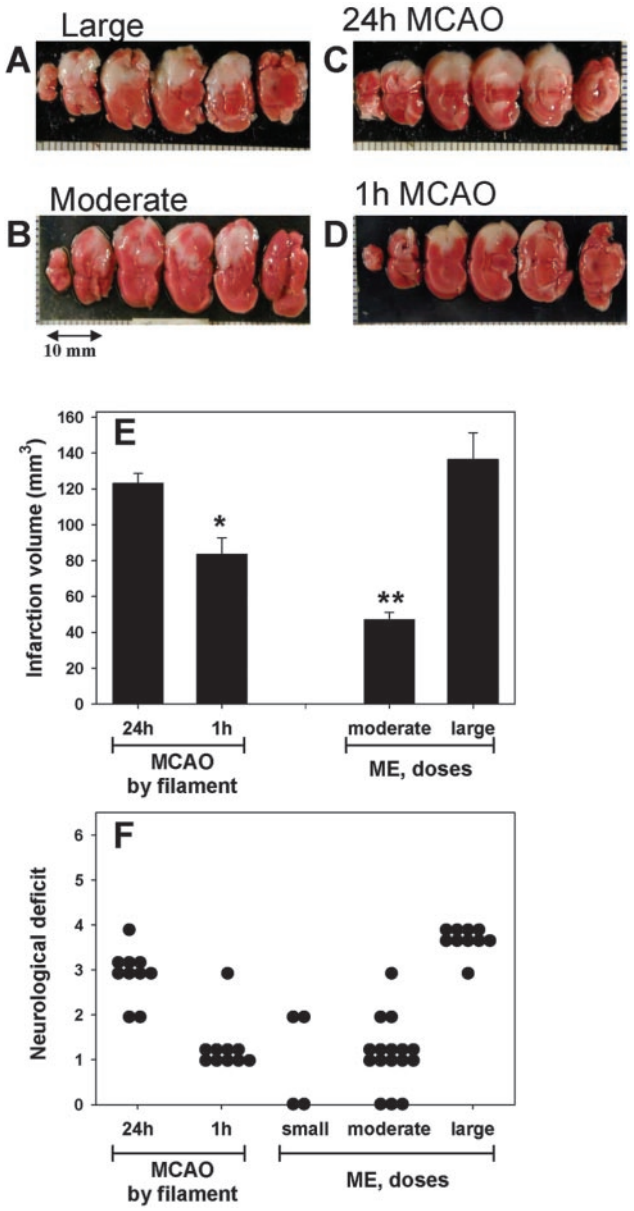

Figure 3. Comparison of microemboli (ME) model with MCAO model. Representative images are shown of TTC-stained coronal brain sections 24 hours after infarct caused by large microemboli dose (A), moderate microemboli dose (B), permanent MCAO (C), and transient MCAO for 1 hour (D). E, Indirect infarct volumes are compared. *$P<0.05$, 1-hour MCAO (n=10) vs 24-hour permanent MCAO (n=10) and vs large dose (n=8); **$P<0.05$, moderate dose (n=16) vs large dose, vs 1-hour MCAO, and vs 24-hour MCAO; F, Neurological scoring in groups as described for E, except small dose is also shown (n=4). Data for 1-hour MCAO, small microemboli dose, and moderate microemboli dose were not significantly different; in contrast, they were significantly different ($P<0.01$) from 24-hour MCAO and large microemboli dose.

Microemboli Dissolution, Reperfusion, and Effect of tPA Knockout

Previous studies showed that microemboli lodged in the pulmonary vasculature spontaneously dissolve within a few hours.[6,7] In contrast, radiolabeled tracing revealed that after initial 40% to 50% dissolution within the first hour, a large dose of ^{125}I-labeled microemboli lodged in the cerebral vasculature failed to resolve completely within 3 hours (Figure 4). These data agree with measurements of blood flow: rCBF remained markedly reduced even several hours after injection of a large dose of microemboli (Figure 2A). This dose caused permanent reduction of ipsilateral rCBF and later reduction of contralateral rCBF (Figure 2A).

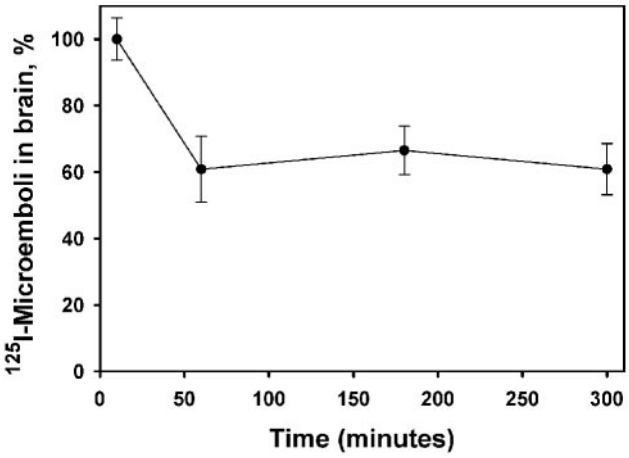

Figure 4. Tracing of spontaneous dissolution of radiolabeled microemboli in the brain. Time course of residual radioactivity recovered in the brain after intracarotid injection of ^{125}I-labeled microemboli is shown; n=6 (10 minutes), n=4 (60 minutes), n=13 (180 minutes), n=3 (300 minutes).

Five minutes after a moderate dose of microemboli, rCBF was reduced to similar levels in WT and tPA$^{-/-}$ mice (Figure 5A). However, tPA$^{-/-}$ mice demonstrated a delay of reperfusion rate measured by LDF within the first 30 minutes compared with WT mice (27.4±5.6 in tPA$^{-/-}$ mice, 56.9±9.6 in WT mice [% baseline]; n=7 each group). By 60 minutes after injection, rCBF returned to normal in WT mice, while it remained significantly depressed in tPA$^{-/-}$ mice. ^{125}I-labeled microemboli tracing revealed that genetic ablation of tPA markedly retarded the rate of thrombi dissolution in the brain (Figure 5B). Infarct volume was significantly greater in tPA$^{-/-}$ mice than in WT mice (Figure 5C), and neurological score revealed a trend to more severe injury (2.0±0.6 in tPA$^{-/-}$ mice [n=4]; 0.97±0.15 in WT mice [n=16]). Mean arterial blood pressure and temperature did not differ between WT and tPA$^{-/-}$ mice.

Discussion

Models of embolic stroke have been used in a variety of animal species, including rabbits, rats, and mice.[5] One type of model involves intravascular occlusion, for example, by filament, ligature, or vessel injury and thrombosis.[11–13] A second type of model involves injection of preformed fibrin or blood clot(s).[3–5] Generally, in these models flow and tissue injury are measured rather than thrombus deposition and dissolution. A third type of model involves embolization of polyvinylsiloxane or microspheres[14,15] that do not resemble blood clots in composition and are not susceptible to fibrinolysis.

In this report we describe a mouse model of stroke that involves the intracarotid injection of microemboli. This model differs from existing embolic models in several im-

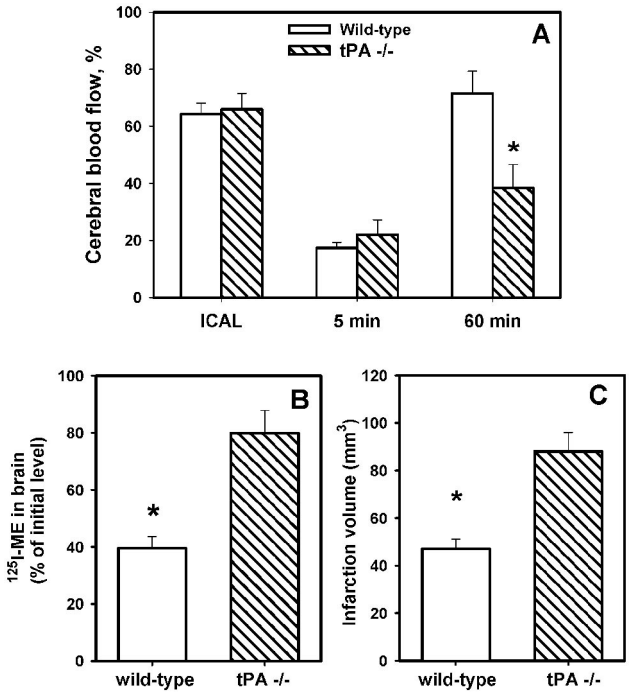

Figure 5. Effect of stroke caused by microemboli in WT and tPA$^{-/-}$ mice. A, rCBF by LDF after carotid artery ligation (ICAL) and 5 and 60 minutes after injection of microemboli in WT (n=12) or tPA$^{-/-}$ (n=7) mice. *P<0.05 vs WT. B, Residual ^{125}I-labeled microemboli in brain of WT (n=4) and tPA$^{-/-}$ (n=3) mice 60 minutes after microemboli injection. *P<0.05 vs tPA$^{-/-}$. C, Infarct volumes 24 hours after injection of microemboli in WT (n=16) and tPA$^{-/-}$ (n=4) mice. *P<0.05 vs tPA$^{-/-}$.

portant ways. First, microemboli are much smaller (2.5 to 3 μm) than previously described clots (varying from 200 μm to millimeters) and reach the microcirculation. Second, this model permits accurate, reproducible, and quantitative determinations of deposition and dissolution of thrombi in vascular beds in mice, a species amenable to genetic manipulations. Third, the extent of cerebral injury can be varied by the dose of microemboli clot burden. Fourth, this model permits evaluation of the role of specific components of blood clots (eg, platelets) in spontaneous and therapeutic dissolution of clot.[7] Here we adapted this model to investigations of cerebral thrombosis, fibrinolysis, and ischemic brain injury.

In this study we used 3 doses of microemboli. At the small dose, the perfusion defect and neurological deficit varied. Conceivably, this dose might represent a model of silent cerebral microembolism seen in the perioperative period ("brain shower"). Moderate doses resulted in a reproducible and transient reduction in rCBF. Blood flow is restored spontaneously, reflecting endogenous fibrinolysis. Therefore, the moderate dose may be appropriate to study thrombosis and endogenous fibrinolysis. High doses of microemboli resulted in reductions in rCBF that did not recover, with larger infarcts and higher mortality. Because there is no spontaneous fibrinolysis, these conditions could be used to study the effects of exogenous plasminogen activators.

To monitor the effect of microemboli on cerebral perfusion, we used 2 complementary methods to assess rCBF: LDF and LSI. LDF is a standard method to follow relative changes in blood flow. LSI is a relatively new technique for dynamic blood flow monitoring that generates a real-time, 2-dimensional cortical surface map of blood flow, with micron spatial resolution and millisecond time resolution. Both LDF and LSI show that moderate doses of microemboli cause transient reductions in rCBF in the MCA territory, followed by spontaneous resolution, while large doses of microemboli cause sustained reductions in blood flow.

Tracing of ^{125}I confirmed incomplete dissolution after a large dose of radiolabeled microemboli: some spontaneous clearance occurs (40% to 50% drop in the first hour), but thereafter the amount of the residual radioactivity in the brain remains relatively constant. A good agreement between flowmetry and radiotracing data validates our observations, since in contrast to LDF or LSI, radiolabeled tracing detects residual microemboli throughout the brain matter including the deep tissues, which may not be reflected in cortical surface measurements.

The microemboli model differs from the MCAO model in several important ways. First, while the microemboli lodge primarily in the distribution of the ipsilateral MCA, detectable amounts are also found in other territories, likely distributed by the circle of Willis to areas supplied by anterior cerebral artery and posterior communicating artery. This differs from the filament model, in which only the MCA territory itself is affected. Second, the microemboli model allows dose-dependent escalation of clot burden, with parallel increases in perfusion impairment, infarct size, and neurological deficit. Third, the microemboli are susceptible to fibrinolysis, and therefore the model can be used to study the effects of endogenous and exogenous plasminogen activators. In contrast, the filament model mainly imitates the reperfusion effect of fibrinolysis (by pulling out the filament after transient MCAO) but not fibrinolysis itself. Fourth, the microemboli model allows us to follow the kinetics of microemboli deposition and dissolution quantitatively, which would not be possible with the filament model.

There have been several studies to date on the role of tPA in ischemic brain injury in mice. In 1 study in which MCAO by filament was used, tPA$^{-/-}$ mice had smaller infarcts, suggesting that tPA may have detrimental effects after cerebral ischemia.[16] In another study in which the MCA was ligated, tPA$^{-/-}$ mice also showed smaller infarcts.[12] In a third study in which MCAO by filament was used, tPA$^{-/-}$ mice showed larger infarcts.[17] In this case, the filament used was known to be thrombogenic, and the increased infarct size was also associated with cerebrovascular fibrin deposition and reduction in rCBF. Finally, in a photochemical vascular injury model, the outcome of tPA$^{-/-}$ mice depended on the severity of injury.[13] Taken together, these studies are consistent with 2 activities of tPA, with opposite effects on infarct size. The first is activation of fibrinolysis that would result in reperfusion and limit infarct size. The second is toxic effects of tPA that would increase infarct size. The net result of these effects depends on the extent to which the models reflect contribution of fibrinolysis to reperfusion; the more they do, the greater is the protective effect of tPA from fibrinolysis.

Our results confirm a role for endogenous tPA in dissolution of cerebral clots in mice. tPA$^{-/-}$ mice show persistence

of reduction in blood flow compared with WT mice, with greater clot burden in the brain and larger infarcts. Future experiments with permanent MCAO in $tPA^{-/-}$ mice will provide further understanding of the role of endogenous tPA in cerebral ischemic injury. In addition, further experiments with radiolabeled microemboli will allow detailed analysis of the role of endogenous tPA in dissolution of microemboli.

In summary, we describe a model of stroke that involves microvascular thrombosis due to the injection of fibrin microemboli. The unique features of this model are (1) the small and uniform size of the microemboli, (2) the ability to modulate the extent of injury by microemboli dose, (3) the sensitivity of the microemboli to fibrinolysis, and (4) the ability to follow deposition and dissolution of microemboli by radiolabeled tracing. This model should be useful to study the role of thrombosis and fibrinolysis in cerebral ischemia.

Acknowledgments

This work was supported by Public Health Service grants R01-NS33335 (P.L.H.), R01-HL66442 (V.R.M.), and P50-NS10828 (M.A.M.), and an American Heart Association Bugher-Stroke Award (V.R.M.).

References

1. Brown WR, Moody DM, Challa VR, Stump DA, Hammon JW. Longer duration of cardiopulmonary bypass is associated with greater numbers of cerebral microemboli. *Stroke*. 2000;31:707–713.
2. Kwiatkowski TG, Libman RB, Frankel M, Tilley BC, Morgenstern LB, Lu M, Broderick JP, Lewandowski CA, Marler JR, Levine SR, Brott T. Effects of tissue plasminogen activator for acute ischemic stroke at one year. National Institute of Neurological Disorders and Stroke Recombinant Tissue Plasminogen Activator Stroke Study Group. *N Engl J Med*. 1999;340:1781–1787.
3. Zhang Z, Chopp M, Zhang RL, Goussev A. A mouse model of embolic focal cerebral ischemia. *J Cereb Blood Flow Metab*. 1997;17:1081–1088.
4. Zhang RL, Chopp M, Zhang ZG, Jiang Q, Ewing JR. A rat model of focal embolic cerebral ischemia. *Brain Res*. 1997;766:83–92.
5. del Zoppo GJ. Relevance of focal cerebral ischemia models: experience with fibrinolytic agents. *Stroke*. 1990;21:IV155–IV160.
6. Bdeir K, Murciano JC, Tomaszewski J, Koniaris L, Martinez J, Cines DB, Muzykantov VR, Higazi AA. Urokinase mediates fibrinolysis in the pulmonary microvasculature. *Blood*. 2000;96:1820–1826.
7. Murciano JC, Harshaw D, Neschis DG, Koniaris L, Bdeir K, Medinilla S, Fisher AB, Golden MA, Cines DB, Nakada MT, Muzykantov VR. Platelets inhibit the lysis of pulmonary microemboli. *Am J Physiol*. 2002;282:L529–L539.
8. Atochin DN, Clark J, Demchenko IT, Moskowitz MA, Huang PL. Rapid cerebral ischemic preconditioning in mice deficient in endothelial and neuronal nitric oxide synthases. *Stroke*. 2003;34:1299–1303.
9. Dunn AK, Bolay H, Moskowitz MA, Boas DA. Dynamic imaging of cerebral blood flow using laser speckle. *J Cereb Blood Flow Metab*. 2001;21:195–201.
10. Huang Z, Huang PL, Panahian N, Dalkara T, Fishman MC, Moskowitz MA. Effects of cerebral ischemia in mice deficient in neuronal nitric oxide synthase. *Science*. 1994;265:1883–1885.
11. Garcia JH, Yoshida Y, Chen H, Li Y, Zhang ZG, Lian J, Chen S, Chopp M. Progression from ischemic injury to infarct following middle cerebral artery occlusion in the rat. *Am J Pathol*. 1993;142:623–635.
12. Nagai N, De Mol M, Lijnen HR, Carmeliet P, Collen D. Role of plasminogen system components in focal cerebral ischemic infarction: a gene targeting and gene transfer study in mice. *Circulation*. 1999;99:2440–2444.
13. Nagai N, Zhao BQ, Suzuki Y, Ihara H, Urano T, Umemura K. Tissue-type plasminogen activator has paradoxical roles in focal cerebral ischemic injury by thrombotic middle cerebral artery occlusion with mild or severe photochemical damage in mice. *J Cereb Blood Flow Metab*. 2002;22:648–651.
14. Yang Y, Yang T, Li Q, Wang CX, Shuaib A. A new reproducible focal cerebral ischemia model by introduction of polyvinylsiloxane into the middle cerebral artery: a comparison study. *J Neurosci Methods*. 2002;118:199–206.
15. Omae T, Mayzel-Oreg O, Li F, Sotak CH, Fisher M. Inapparent hemodynamic insufficiency exacerbates ischemic damage in a rat microembolic stroke model. *Stroke*. 2000;31:2494–2499.
16. Wang YF, Tsirka SE, Strickland S, Stieg PE, Soriano SG, Lipton SA. Tissue plasminogen activator (tPA) increases neuronal damage after focal cerebral ischemia in wild-type and tPA-deficient mice. *Nat Med*. 1998;4:228–231.
17. Tabrizi P, Wang L, Seeds N, McComb JG, Yamada S, Griffin JH, Carmeliet P, Weiss MH, Zlokovic BV. Tissue plasminogen activator (tPA) deficiency exacerbates cerebrovascular fibrin deposition and brain injury in a murine stroke model: studies in tPA-deficient mice and wild-type mice on a matched genetic background. *Arterioscler Thromb Vasc Biol*. 1999;19:2801–2806.

Mouse Model of Microembolic Stroke and Reperfusion

D.N. Atochin, J.C. Murciano, Y. Gürsoy-Özdemir, T. Krasik, F. Noda, C. Ayata, A.K. Dunn, M.A. Moskowitz, P.L. Huang and V.R. Muzykantov

Stroke. 2004;35:2177-2182; originally published online July 15, 2004;
doi: 10.1161/01.STR.0000137412.35700.0e
Stroke is published by the American Heart Association, 7272 Greenville Avenue, Dallas, TX 75231

Print ISSN: 0039-2499. Online ISSN: 1524-4628